The effect of volatile organic acids and CO_2 on the corrosion rate of carbon steel from a Top-of-Line-Corrosion (TLC) perspective

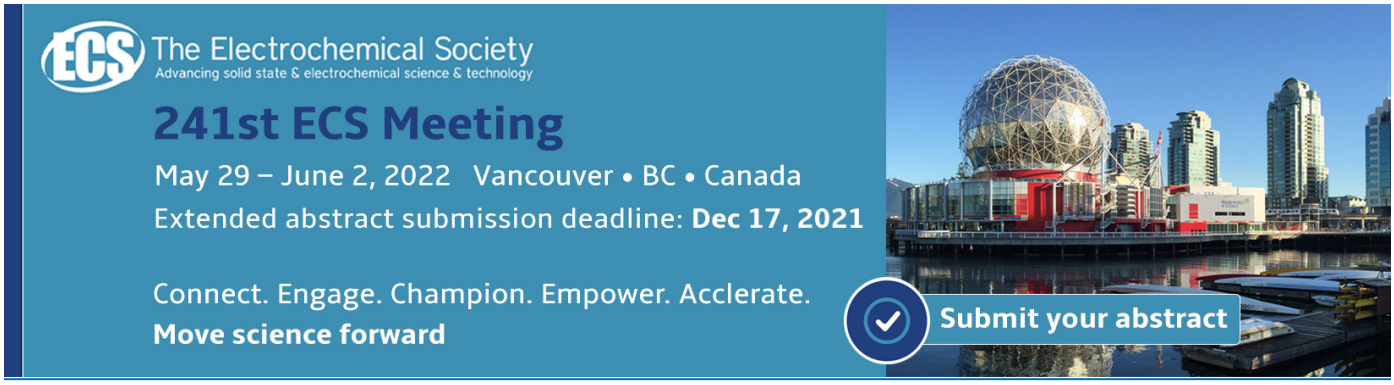

The effect of volatile organic acids and CO_2 on the corrosion rate of carbon steel from a Top-of-Line-Corrosion (TLC) perspective

S B Gjertsen[1, 2,*], A Palencsar[1], M Seiersten[1], T H Hemmingsen[2]

[1] Institute for Energy Technology
[2] Faculty of Science and Technology, University of Stavanger, Norway

[*] Contact author: sondre.gjertsen@ife.no

Abstract. Models for predicting top-of-line corrosion (TLC) rates on carbon steels are important tools for cost-effectively designing and operating natural gas transportation pipelines. The work presented in this paper is aimed to investigate how the corrosion rates on carbon steel is affected by acids typically present in the transported pipeline fluids. This investigation may contribute to the development of improved models. In a series of experiments, the corrosion rate differences for pure CO_2 (carbonic acid) corrosion and pure organic acid corrosion (acetic acid and formic acid) on X65 carbon steel were investigated at starting pH values; 4.5, 5.3, or 6.3. The experiments were conducted in deaerated low-salinity aqueous solutions at atmospheric pressure and temperature of 65 °C. The corrosion rates were evaluated from linear polarization resistance data as well as mass loss and released iron concentration. A correlation between lower pH values and increased corrosion rates was found for the organic acid experiments. However, the pH was not the most critical factor for the rates of carbon steel corrosion in these experiments. The experimental results showed that the type of acid species involved and the concentration of the undissociated acid in the solution influenced the corrosion rates considerably.

1. Introduction

Over the last two decades, the interest in top-of-line corrosion (TLC) has increased in the oil and gas industry [1]. TLC is a form of corrosion occurring typically in submerged wet gas transportation pipelines. The ocean's cooling effect on the pipeline's flowing fluid causes transported vapor to condense onto the pipe wall. In a stratified flow regime, typical for wet gas transport, droplets will condense from the vapor at contact with the colder steel surface. The wetting of the internal pipe wall establishes electrochemical cells at the steel surface, and condensed water together with acids plays the role of corrosive medium. Due to gravity, the top-of-line droplets drain or drop off the wall to the pipeline's bottom-of-line and cumulate with the fluid stream there. The process continues, and new droplets may constantly replace the old drained-off ones. The absence of salts in freshly condensed water can result in a very acidic pH [2]. For wet gas pipelines, a pH below 4 is typical before the condensed water is affected by the iron ions (Fe^{2+}) dissolving from the corrosion reaction [3]. Hinkson et al. reported a pH of 3.3 in freshly condensed water from modeling the condensate composition in a pipeline scenario [4]. For a much-used TLC rate prediction model [5], pH is essential for assessing the Fe^{2+} solubility. Supersaturation with Fe^{2+} and precipitation of protective scales on the steel surface that slows down the

corrosion process is difficult to achieve with a higher Fe^{2+} solubility. Hence, increased Fe^{2+} solubility will yield higher predicted corrosion rates (CR). Before iron supersaturation in the condensed top-of-line aqueous phase, the corrosion process results in the following (generalized) heterogeneous reaction:

$$Fe_{(s)} + 2H^{+}_{(aq)} \rightarrow Fe^{2+}_{(aq)} + H_{2\,(g)} \quad (1)$$

The presence of weak acids strongly influences the cathodic part of this reaction. Carbon dioxide (CO_2) and organic acids that dissolve or co-condense with the liquid phase onto the pipe wall are known to increase corrosion rates of carbon steel [6, 7]. Dissolved CO_2 has an acidifying effect on the aqueous solution as carbonic acid (H_2CO_3) is formed by hydration. H_2CO_3 is a source of hydrogen ions (H^+) by dissociation to bicarbonate ion (HCO_3^-) and further to carbonate (CO_3^{2-}) [7]. Acetic acid with the formula CH_3COOH (HAc) and formic acid with the formula HCOOH (HFo) are two of the most common organic acids in oil and gas reservoirs. The mentioned weak acids affect the aqueous solution acidity by the following equilibrium reactions:

$$H_2O_{(l)} + CO_{2\,(aq)} \rightleftharpoons H_2CO_{3\,(aq)} \rightleftharpoons HCO_3^-{}_{(aq)} + H^+{}_{(aq)} \rightleftharpoons CO_3^{2-}{}_{(aq)} + 2H^+{}_{(aq)} \quad (2)$$

$$CH_3COOH_{(aq)} \rightleftharpoons CH_3COO^-{}_{(aq)} + H^+{}_{(aq)} \quad (3)$$

$$HCOOH_{(aq)} \rightleftharpoons HCOO^-{}_{(aq)} + H^+{}_{(aq)} \quad (4)$$

The present study aims to clearly state whether the corrosion rate correlates directly with pH or not. If not, it is relevant to investigate how pH and different weak acids affect the corrosion rate. Garsany et al. concluded in their study that for CO_2 corrosion in petroleum pipelines, the critical factor is the concentration of the undissociated acid when anions from weak acids are present in the aqueous medium and not the pH [8]. Several studies on organic acid's effect on CO_2 corrosion with similar reports have been conducted [6, 9, 10]. It is essential to understand how weak acids affect the pH differently in order to understand how weak acids affecting carbon steel corrosion rate. HAc is often referred to as a stronger acid than carbonic acid in the CO_2 corrosion literature [10, 11], but H_2CO_3 has a higher pK_a for the dissociation to HCO_3^- than HAc [12]. Table 1 lists the pK_a values for the acids investigated in this study. According to Henry's law, the equilibrium concentration of H_2CO_3 in water will primarily be determined by the CO_2 gas partial pressure ($pCO_{2\,(g)}$).

In an investigation on HAc's influence on CO_2 corrosion of carbon steel, George and Nesic reported accelerated corrosion rates for increasing HAc concentrations, although the pH was maintained at 4 [6]. HAc's influence on the corrosion rate was more pronounced when the temperature was increased from 22 °C to 60 °C. A doubling in the corrosion rates was reported when the HAc concentration was changed from 0 to 85 ppm at 60 °C. Okafor et al. reported similar temperature dependency for HAc's influence on corrosion rate at 80 °C [10]. The latter two studies report a shift from charge-transfer control of the corrosion rate at room temperature (22 °C) to mass-transfer limiting current controlled at higher temperatures. Experiments by Amri et al. and Kahyarian et al. suggest that HAc acts as a local reservoir of protons near the corroding metal surface rather than participating electroactive in the cathodic part of the corrosion process [3, 13]. It is worth mentioning the investigation on whether acetic acid contributes to increased corrosion rates through the *homogenous* reaction by *buffering* H^+ at the corroding surface or *heterogeneous* reaction by *direct reduction* [3, 10, 13]. When talking about TLC, it is useful to keep in mind that the conditions in these studies do not favor passivation and show corrosion rates far higher than expected in the field.

Table 1. pKa of the investigated acids

Acid	Carbonic	Acetic	Formic
Formula	H_2CO_3	CH_3COOH	HCOOH
pK_{a1} at 25°C	3.6 (HCO_3^-)	4.76	3.75
pK_{a2} at 25°C	6.35 (CO_3^{2-})		

2. Experimental Procedure

3L glass cells were used for setting up electrochemical cells with two carbon steel specimens serving as working electrodes in a conventional three-electrode configuration for electrochemical measurements. The electrode arrangement consisted of a silver/silver chloride (Ag/AgCl) reference electrode with a 3 M potassium chloride (KCl) internal solution and a coiled platinum (Pt) wire as a counter electrode. The Pt counter electrode had a significantly larger surface areal than the working electrodes. The examined material was *API X65* carbon steel from the *Ormen Lange* pipeline. The chemical composition is presented in Table 2. Two samples of the examined material were working electrodes for corrosion rate measurements in each experiment; they were connected to a *Gamry® PCI4* potentiostat via a *Gamry® ECM8* multiplexer. The test samples were machined cylinders with 10 mm in diameter and 10 mm in height, threaded between two *Teflon®* separators onto *PEEK*-covered sample holders providing electrical connection; the exposed steel area of each working electrode was 3.14 cm^2.

Table 2. Chemical Composition of *API X-65* Steel in wt%

C	Si	Mn	S	P	Cr	Ni	V	Mo	Cu	Al	Sn	Nb
0.087	0.26	1.57	0.007	0.014	0.015	0.116	0.058	0.001	0.122	0.003	0.003	0.024

After assembly of the apparatus, electrolytes of the required composition given in Table 3 were prepared. In the table, the CO_2 experiments are referenced with the letter C and the experiment's pH value. For the HAc experiments the letter A is used, and the letter F is assigned to the HFo experiments. The total concentration of acid and its conjugated base was ca. 0.5 M in the HAc and HFo experiments (A(pH) and F(pH)). In the CO_2 experiments (C(pH)), carbonic acid was produced in the solutions by water's hydration of dissolved CO_2. The relatively high concentration of organic acid species was selected to reduce the effect of consumption, maintaining a relatively constant level similarly to the carbonic acid tests where CO_2 was constantly resupplied by bubbling. This strategy was applied to mimic the continuous condensation scenario where all acid species may be continuously resupplied. The test solutions were prepared with technical-grade chemicals dissolved in distilled water. In addition, 1g/kg (0.017M) of sodium chloride (NaCl) was added to the solutions as a base concentration for increased solution conductivity. The electrolytes were deoxygenated by purging CO_2 gas or nitrogen (N_2) gas for at least 1 h. The solution temperature was 65 °C, and a hot plate connected to a thermocouple heated and kept the solution at a stable temperature. The outlet gas was cooled in a reflux condenser before going through a water lock to prevent excessive evaporation of the volatile electrolyte species. A pH electrode and a thermocouple, calibrated with two buffer solutions, monitored the solution pH. Before placing the test samples into the test solution, they were abraded with P500 and then P1000 silicon carbide paper, cleaned in an ultrasonic bath with acetone for 10 minutes, dried, and weighed. The samples were dried in a heating cabinet at 50 °C before weighing. Isopropanol was used for rinsing between each step. The test solution had a stable temperature and pH when the sample holders with the prepared samples got inserted into the test cell, and the experiment started.

Once a day, potentiodynamic polarization curves were obtained starting with a cathodic sweep from the open circuit potential (OCP) to -250 mV vs. OCP, followed by an anodic sweep from OCP to +150 mV vs. OCP. The scan rate was 0.1 mV/s. Solution resistance obtained from Electrochemical Impedance

Spectroscopy (EIS) was used to correct for the ohmic drop. EIS was conducted from 200 kHz to 100 mHz with 10 mV rms sinusoidal perturbation around OCP. Corrosion rate measurements were performed using the linear polarization resistance (LPR) technique every 30 min. LPR was performed at -5 mV to 5 mV from OCP with a scan rate of 0.1 mV/s. The iron concentration in samples taken from the test solution was measured with a spectrophotometer twice daily. The concentration values were used to calculate the amount of Fe^{2+} released by the corrosion of the two specimens between the times of sampling, which allowed the average corrosion rate for the respective period to be determined. The experiments lasted from two to four days. The experiments ended by taking the test samples out of the glass cell and rinsing them with isopropanol before placing them in the heating cabinet. After drying for 5 min, the samples were weighed for weight loss (WL) measurements. Corrosion products that may have formed on the specimen surfaces were for the time being preserved for examination; therefore, the mass loss may not be entirely accurate. However, the error is assumed to be relatively small due to the high observed corrosion rates and the unfavorable conditions for, e.g., iron carbonate formation. Key information of the experimental setup in this study are summarized and presented in Table 4.

Table 3. Experimental matrix with concentrations of salt and acids in the test solutions, type of purging gas, and experiment start pH values calculated with the software Multiscale®.

Concentration in solution given in mg/kg								
Experiment no.	NaCl	$NaHCO_3$	$NaCH_3COO$	CH_3COOH	NaHCOO	HCOOH	Bubble gas	Ca. pH @65 °C
C4.5	1000	0	0	0	0	0	CO_2	4.5
C5.3	1000	101					CO_2	5.3
C6.0	1000	588					CO_2	6.0
A4.5	1000		14800	19200			N_2	4.5
A5.3	1000		32000	6600			N_2	5.3
A6.0	1000		39000	1500			N_2	6.0
F4.5	1000				29900	2800	N_2	4.5
F5.3	1000				33300	460	N_2	5.3
F6.0	1000				33900	92	N_2	6.0

Table 4. Key experimental parameters

Steel type	API X-65 carbon steel
Solution type	Oxygen-free distilled water with 0.1 wt% NaCl
Purging gas	CO_2 or N_2
Total pressure	Atmospheric
Start pH	4.5, 5.3 or 6.0
Temperature	65°C
Solution flow	Magnetic stirring and gas bobbling
Measurement techniques	Spectrophotometric Determination of Iron, LPR, potentiodynamic sweeps, EIS, and WL

3. Results and discussion

In the context of the purpose of these experiments, the results show that corrosion rates do not correlate directly with pH regardless of acid type. In this study, experiments with three different pH values, 4.5, 5.3, and 6.0 in deaerated solutions with 0.1 wt% NaCl at 65 °C were carried out. The average corrosion rates calculated from specimens WL for pure CO_2 corrosion and organic acid corrosion without CO_2, are presented in Figure 1. Data from at least four steel specimens have been used in the calculations. The average corrosion rates were approximately twenty times higher at most for the experiments with organic acids than for pure CO_2 corrosion when comparing them at pH 4.5. This is in agreement with the conclusion made by Garsany et al. that the concentration of weak acids in the solution is more critical for the corrosion rate than the pH value [8]. The total concentration of undissociated acid and the conjugate base anion was much higher for the experiments with organic acids than for the CO_2 experiments. However, the pH value is not unessential for the corrosion rate because with decreasing pH values, the acid equilibrium reactions 2, 3, and 4 shift towards the left according to Le Chatelier's principle. Lower pH values lead to higher shares of the total acid to be in the undissociated form. Table 5 shows the concentrations of undissociated acid predicted at the experiment starts by the software Multiscale®. The H_2CO_3 is calculated from the predicted dissolved CO_2 concentrations form Multiscale® with the hydration constant [14].

Table 5. Concentrations of undissociated acid at the experiment starts from calculations in the software Multiscale®.

	Concentrations (mmol/kg)			
pH	CO_2	H_2CO_3	CH_3COOH	HCOOH
4.5	11.68	0.03	284.27	55.94
5.3	11.68	0.03	97.77	9.32
6.0	11.68	0.03	22.21	1.86

For all the different weak acids in this study, the corrosion rates increased when the solutions had lower starting pH. The HFo experiments showed the most substantial increase in corrosion rate with decreasing pH. With a change in pH from 6.0 to 4.5, an increase in the corrosion rate of approximately 20 times was observed. The corrosion rates seen in the HAc experiments did also increase considerably from pH, 6.0 to 4.5. A minor increase did also occur for the CO_2 experiments, where the solutions had a continuous supply of acid by purging the solutions with CO_2 gas and hydration of the solved CO_2. Thus, if the hydration reaction is fast enough, the acid supply in the CO_2 experiment solutions can be assumed to be nearly constant over time. In the organic acid experiments, the effect of consumption was counteracted by the high initial concentrations. The total amount of acids and conjugate bases were added in the organic acid experiments before the experiments started. To compare the effect of the different weak acids on corrosion rate, one should remember that the different solutions had very different acid concentrations, which affects solution activity and the kinetics of the reactions. HFo was added in relatively small quantities to the solutions due to its strong effect on pH. HFo is the strongest of the two organic acids in this study. Hence, the HFo experiments had smaller concentrations of undissociated acid than the HAc experiments. Still, the highest corrosion rate in this study was seen for experiments with HFo at pH 4.5 (F4.5).

Due to the experimental design, the total concentration of acid and the conjugate base was set to 0.5 M for all the organic acid experiments. The HFo experiments had higher concentrations of sodium (Na). The conjugate bases were added to the solutions as their Na salt. Therefore, the HFo experiments had the highest ionic strength; this may have contributed to a disproportionate increase in the corrosion rates compared to the HAc experiments. Even though a more fundamental analysis of possible mechanisms is yet to be done, one may speculate if higher mobility of smaller formate ions affects if mass-transfer

limitations play a role. The CO_2 experiments had the lowest ionic strength. The highest corrosion rate was seen for F4.5, although that experiment did not have the highest concentration of undissociated acid. The corrosion rates measured by LPR at 5 h from the start of the experiments are presented in Figure 2. These results are consistent with the average WL corrosion rates. A notable difference of lower corrosion rates measured at 5 h than the average WL calculated corrosion rates could be observed for the CO_2 and HAc experiments. For the HFo experiments, the trend was the opposite, and corrosion rates decreased over time. Over time, the decreasing corrosion rate in the HFo experiments can most likely be explained by the consumption of undissociated acid and HFo's poorer buffer capacity. The development in corrosion rates over time can be seen more easily in Figure 3, which shows the LPR measured corrosion rates. 5 h has been marked with a red line in the figure. The "carbide effect" may explain the increasing corrosion rates over time in the CO_2, and HAc experiments [15, 16].

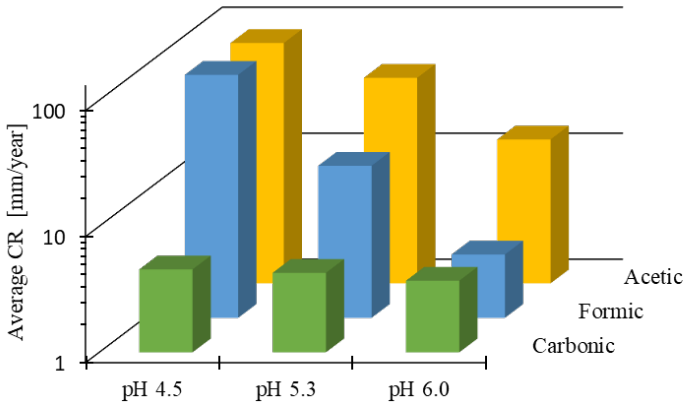

Figure 1. Average corrosion rates calculated from sample WL for all experiments.

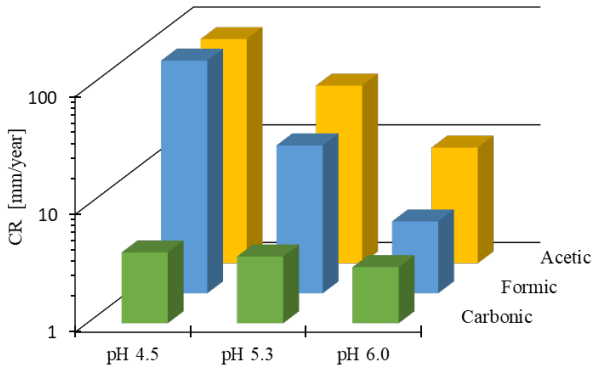

Figure 2. Corrosion rates measured with LPR at 5 h from the start of the experiments.

Although the same effect applies for the HFo experiments, the corrosion rates decrease over time due to a more pronounced effect from the acid consumption. When the iron specimens undergo corrosion, iron carbide (Fe_3C) in the steel microstructure will remain at the corroded surface while the iron around dissolves. The Fe_3C is a conductor, and its surface can serve as an additional area for the cathodic reaction to occur. Hence, the area for the cathodic reaction increases and speeds up the anodic dissolution reaction. A Fe_3C film left on the iron surfaces can explain the visually observable surface changes of the steel specimens in all experiments. Within a minute after submerging the specimens into the solution, their surfaces changed from shiny to matte. All the surfaces had turned completely black after 5 hours into the experiments. When the specimens were extracted from the cell and rinsed in isopropanol, black particles were easily washed off, and "iron grey" surfaces were uncovered. The present investigation reports corrosion rates far higher than expected and experienced for TLC field

cases, which is typically well below 1 mm/year [17]. For wet gas pipelines in operation, the corrosion rate is expected to slow down over time due to the precipitation of protective scales like iron carbonate ($FeCO_3$). The experiments were designed to study corrosion in the active dissolution range and not the precipitation mechanism. There was no evidence of protective scale precipitation in the corrosion rate measurements or the development of measured iron concentration. All the reported results have been from active corrosion processes.

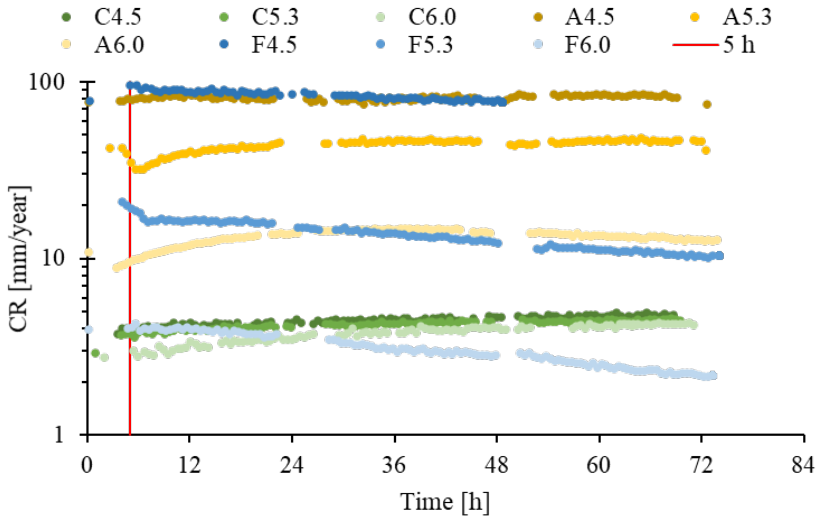

Figure 3. CR measured from LPR for all experiments. The red line marks 5 h.

For the experiments with carbonic acid at pH 4.5 (C4.5), the solution had no other salt than the base concentration of 1wt% NaCl added. The measured solution pH of C4.5 was in agreement with the calculations done in the software Multiscale® and stabilized between 4.1 and 4.2 before the experiment started. The measured pH values for all experiments are presented in Figure 4. Except for C4.5, the pH in the other experiments increased linearly over time. In the first hours, C4.5 had a more rapid increase due to the low alkalinity. The increase was almost linear after 48 h. The rapid pH increase early in C4.5 is relevant when assessing these experiments concerning the low salinity of freshly condensed water in TLC. Except for C4.5, pH increases most rapidly in the HFo experiments, although carbonic acid is the strongest. The development in pH cannot be justly compared between the CO_2 and organic acid experiments due to the continuous resupply of carbonic acid. HFo's position as a stronger weak acid, and therefore has a poorer buffer capacity than HAc, was in agreement with the development of measured pH in the organic acid experiments.

Figure 5 shows corrosion rates measurements from both LPR and spectrophotometric determination of iron for A4.5. Again, the observed correlation between the two methods for measuring corrosion rate was reasonable. This trend applies to all the experiments.

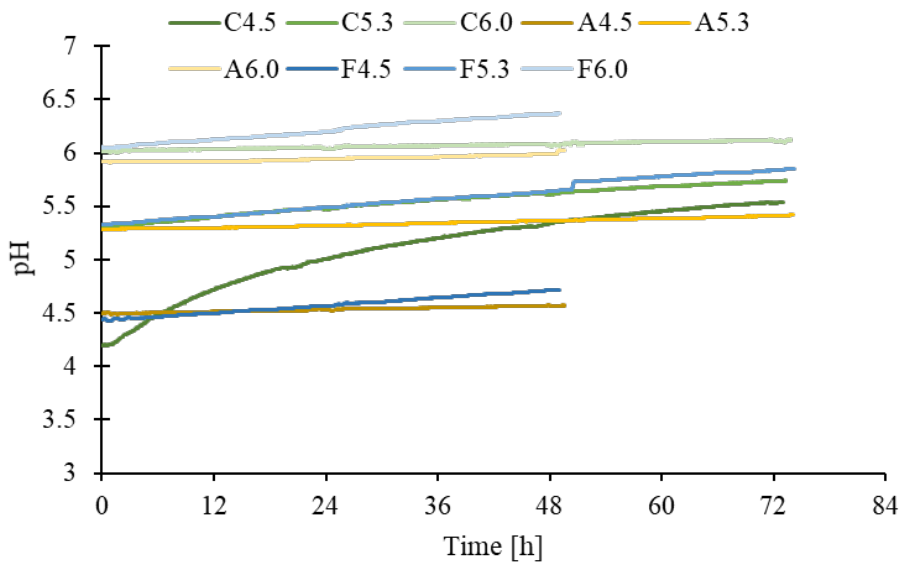

Figure 4. CR measured from LPR for all experiments. The red line marks 5 h.

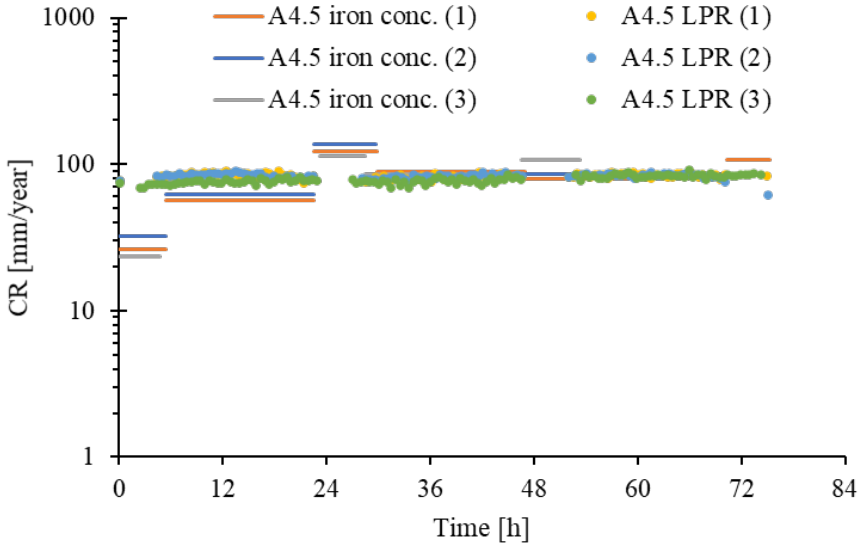

Figure 5. Comparison of CR measurements by LPR and iron concentration spectrophotometry for the experiments with HAc and pH 4.5 (A4.5).

4. Conclusion

For oxygen-free solutions at 65 °C, the following was found:

- The corrosion rates evaluated from the different techniques, linear polarization resistance (LPR) data, mass loss, and released iron concentration correlated well, which gives the reported results a good level of confidence.
- In the presence of weak acids, pH is not the most critical parameter for active corrosion rates in TLC. The concentration and type of weak acid had a more pronounced influence on corrosion rate.
- The highest corrosion rate in this study was seen for formic acid at low pH (4.5).

- When the total concentration of organic acid and its conjugate base is kept at the same level, the corrosion rate decreases when the ratio shift towards less undissociated acid.
- The mechanisms governing the corrosion process and its rate for active TLC appear to be complex and further analysis of the collected data is required.

Acknowledgment: This work has been carried out in an ongoing Ph.D. study in the project ModTLC at IFE and UiS in Norway. ModTLC is a joint industrial project, and the authors would like to acknowledge the financial support from the members, Equinor ASA and A/S Norske Shell, as well as The Research Council of Norway.

References

[1] Al-Moubaraki A H, Obot I B 2021 Top of the line corrosion: causes, mechanisms, and mitigation using corrosion inhibitors. *Arabian J Chem*. **14**(5),103116.
[2] Singer M 2017 16 - Top-of-the-line corrosion. In: El-Sherik AM, editor. *Trends in Oil and Gas Corrosion Research and Technologies*. Boston: Woodhead Publishing, p. 385-408.
[3] Amri J, Gulbrandsen E and Nogueira R P 2011 (ed.) Role of acetic acid in CO_2 Top of the Line Corrosion of carbon steel. *Corros.* 2011 NACE-11329.
[4] Hinkson D, Zhang Z, Singer M and Nesic S 2010 Chemical composition and corrosiveness of the Condensate in Top-of-the-Line Corrosion. *Corros.* **66**(4), 045002--8.
[5] Nyborg R, and Dugstad A 2007 (ed.) Top of line corrosion and water condensation rates in wet gas pipelines. *Corros.* 2007. NACE-07555.
[6] George K S, Nesic S 2007 Investigation of carbon dioxide corrosion of mild steel in the presence of acetic acid - Part 1: Basic mechanisms. *Corros*. **63**(2), 178-86.
[7] Kahyarian A, Achour M and Nesic S 2017 7 - CO_2 corrosion of mild steel. In: El-Sherik AM, editor. *Trends in Oil and Gas Corrosion Research and Technologies*. Boston: Woodhead Publishing, p. 149-90.
[8] Garsany Y, Pletcher D and Hedges B 2002 Speciation and electrochemistry of brines containing acetate ion and carbon dioxide. *J Electroanal Chem*. **538-539**, 285-97.
[9] Fajardo V, Canto C, Brown B and Nesic S 2007 (ed.) Effect of organic acids in CO_2 corrosion. *Corros*. 2007. NACE-07319.
[10] Okafor PC, Brown B and Nesic S 2009 CO_2 corrosion of carbon steel in the presence of acetic acid at higher temperatures. **39**(6), 873-7.
[11] Srdjan N 2007 Key issues related to modelling of internal corrosion of oil and gas pipelines – A review. *Corros. Sci.* **49**(12), 4308-38.
[12] Dugstad A 2015, editor Fundamental aspects of CO2 metal loss corrosion, Part I: mechanism. *Corros.* 2015. NACE-2015-5826.
[13] Kahyarian A, Schumaker A, Brown B and Nesic S 2017 Acidic corrosion of mild steel in the presence of acetic acid: Mechanism and prediction. *Electrochim Acta*. **258**, 639-52.
[14] Nordsveen M, Nesic S, Nyborg R and Stangeland A 2003 A mechanistic model for carbon dioxide corrosion of mild steel in the presence of protective iron carbonate films - Part 1: Theory and verification. *Corros.* **59**(5), 443-56.
[15] Crolet J, Olsen S and Wilhelmsen W 1994 (ed.) Influence of a layer of undissolved cementite on the rate of the CO_2 corrosion of carbon steel. *Corros./*94; Houston, TX: NACE1994.
[16] Berntsen T, Seiersten M and Hemmingsen T 2003 Effect of $FeCO_3$ supersaturation and carbide exposure on the CO2 corrosion rate of carbon steel. *Corros.-Us*. **69**(6), 601-13.
[17] Andersen T R, Halvorsen A M K, Valle A and Dugstad A 2007 (ed.) The Influence of condensation rate and acetic acid concentration on tol-corrosion in multiphase pipelines. *Corros.* 2007. NACE-07312.